UC San Diego

UC San Diego Previously Published Works

Title

Theoretical analysis and optimization of ultrashort echo time (UTE) imaging contrast with off-resonance saturation

Permalink

https://escholarship.org/uc/item/6gj5f27q

Authors

Carl, Michael
Ma, Yajun
Du, Jiang

Publication Date

2018-07-01

DOI

10.1016/j.mri.2018.03.002

Peer reviewed

eScholarship.org Powered by the California Digital Library
University of California

Magnetic Resonance Imaging 50 (2018) 12–16

Contents lists available at ScienceDirect

Magnetic Resonance Imaging

journal homepage: www.elsevier.com/locate/mri

Technical note

Theoretical analysis and optimization of ultrashort echo time (UTE) imaging contrast with off-resonance saturation

Michael Carl[a,*], Yajun Ma[b], Jiang Du[b]

[a] GE Healthcare,United States
[b] Radiology Department, University of California, San Diego, United States

ARTICLE INFO

Keywords:
Off-resonance saturation
Ultrashort echo time (UTE)
Cones
Short T2 contrast

ABSTRACT

Purpose: Off-resonance saturation (ORS) is a tool which can be used in ultrashort echo time (UTE) magnetic resonance imaging to selectively reduce short T2 signals. When these ORS prepared UTE images are subtracted from a non-suppressed UTE acquisition, the short T2 signals are highlighted. The aim of this paper is to develop a theoretical ORS model and optimize short T2 contrast.
Theory: Using a theoretical model the sequence parameters such as saturation flip angle and off-resonance frequency were optimized to maximize short T2 contrast. Bloch simulations were performed to demonstrate the accuracy of the theoretical model.
Methods: Volunteer imaging was performed on the knee using different saturation flip angles and off-resonance frequencies using a Fermi RF pulse with a 3D UTE Cones acquisition.
Results: The off-resonance saturation method showed good long T2 suppression, and highlighted short T2 signals such as the patella tendon. The theoretical signal curves generally agreed with simulated and experimentally measured signals.
Conclusion: Off-resonance saturation 3D UTE imaging can be used to effectively suppress long T2 signals and highlight short T2 signals. Theoretical modeling can be used to optimize sequence parameters to maximize long T2 suppression and short T2 contrast. Experimental results confirmed the theoretical predictions.

1. Introduction

Direct imaging of tissues such as tendons, ligaments, and cortical bone which have short T2 has become possible with the development of ultrashort echo time (UTE) sequences [1–4]. Conventional UTE images are typically proton density or T1 weighted. Since signal is detected from almost all tissues irrespective of their T2 values, the images often lack useful contrast. Off resonance saturation (ORS) or magnetization transfer (MT) prepared UTE imaging provides a method to generate contrast between the short T2 and the surrounding long T2 tissues [5–10]. With ORS, an off-resonance radiofrequency (RF) pulse is applied prior to the UTE imaging sequence in order to selectively reduce signals from the short T2 components since they have broader spectral widths and are therefore saturated by the off-resonance RF pulse. The long T2 components have much narrower spectral widths, and are minimally affected by the off-resonance RF pulse. Positive short T2 contrast can then be achieved by subtracting these images from equivalent UTE acquisition without ORS [5]. Here we develop a simple quantitative theoretical model to optimize the short T2 contrast. In addition, we show that this model can be used to fit the experimental data to calculate the T2 for short T2 tissues.

1.1. Theory

Features of the pulse sequence used in this study are shown in Fig. 1A. The off-resonance saturation pulse is repeated every TR period, after which data from N separate k-space spokes, separated by equal time interval τ, is acquired. Bloch simulations were employed to study the magnetization saturation caused by off-resonance RF pulses. Our simulation model is based on propagating the x,y,z magnetization during small 1 μs time steps during the application of RF pulses, off-resonance, and T1 & T2 decay. Off-resonance, and RF applications were simulated by simple infinitesimal rotations around the z-axes, and x-axes, respectively, while T2/T1 decay/recovery were modeled directly from the corresponding differential Bloch equation terms. With the application of an off resonance saturation RF pulse with a flip angle of θ_{ORS}, our simulations show that the rate of saturation of the z-magnetization is given by:

* Corresponding author at: GE Healthcare, 408 Dickinson Street, San Diego, CA 92103-8226, United States.
E-mail address: Michael.carl@ge.com (M. Carl).

https://doi.org/10.1016/j.mri.2018.03.002
Received 24 December 2017; Received in revised form 5 March 2018; Accepted 7 March 2018
0730-725X/ © 2018 Elsevier Inc. All rights reserved.

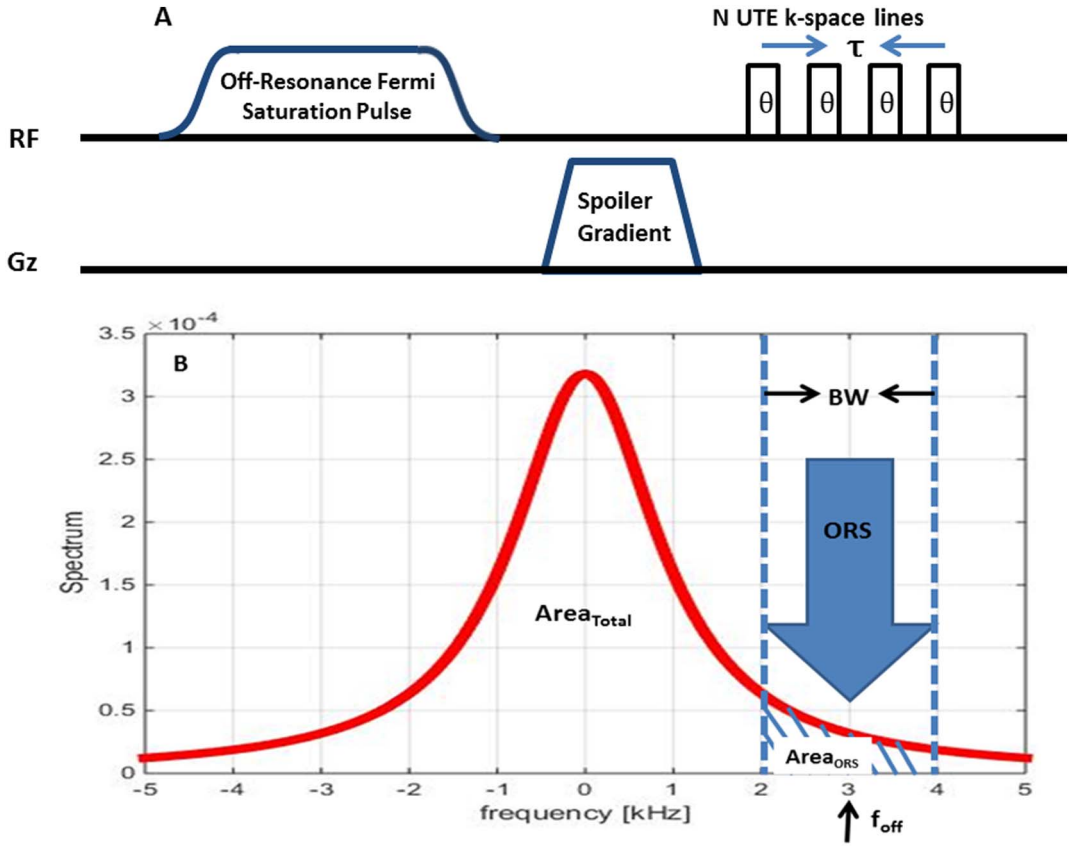

Fig. 1. A) Pulse sequence diagram for ORS prepared UTE sequence. B) Schematic diagram of Lorenzian spectrum for T2 = 1 ms spins and an ORS pulse with a 2 kHz BW (chosen much larger for this diagram for clarity) and 3 kHz off-resonance frequency.

$$\frac{dM_z}{d\theta_{ORS}} = -\alpha\ \theta_{ORS}\, M_z \tag{1}$$

leading to a Gaussian attenuation with respect to θ_{ORS}:

$$M_z = M_0\ exp\left(-\frac{\alpha\ \theta_{ORS}^2}{2}\right) \tag{2}$$

The proportionality constant α which determines the saturation efficiency can be calculated by the spectral area covered by the off-resonance RF pulse divided by the total spectral area (see Fig. 1B). Qualitatively this implies that the saturation rate increases as the RF bandwidth (BW) is increased or as the RF off resonance frequency (f_{off}) is brought closer to the resonance frequency of the spins, as would be expected.

One can calculate a quantitative expression of the area covered by the ORS pulse by using the Lorenzian line-shape:

$$\alpha \equiv \frac{Area_{ORS}}{Area_{Total}} = Area_{ORS} \tag{3}$$

The last step assuming that the line shape is properly normalized (i.e. $Area_{Total} = 1$). The expression for $Area_{ORS}$ can be directly calculated by integrating the normalized line shape over the bandwidth covered by the ORS pulse:

$$\begin{aligned} Area_{ORS} &= \frac{2}{T_2}\int_{foff-BW/2}^{foff+BW/2} \frac{df}{\frac{1}{T_2^2} + (2\pi f)^2} \\ &= \frac{1}{\pi}\left[\text{atan}\left(2\pi T_2\left(f_{off} + \frac{BW}{2}\right)\right) - \text{atan}\left(2\pi T_2\left(f_{off} - \frac{BW}{2}\right)\right)\right] \\ &\approx \frac{2T_2 BW}{1 + (2\pi f_{off}\, T_2)^2} \end{aligned} \tag{4}$$

Eq. (4) implies that for typical ORS experimental conditions, the saturation rate increases for shorter T2 tissues, up to a point where the T2 is so short and the spectrum is so broad/flat that only a small fraction is covered by the ORS pulse BW. Taking the derivative of Eq. (4) with respect to T2 and setting it to zero results in an expression for the threshold T2 for maximum saturation, such that shorter T2 experience less efficient saturation:$T2_{threshhold} = 1/(2\pi f_{off})$. For experimental conditions typically encountered in ORS imaging (e.g. $f_{off} > 1$ kHz) this yields $T2_{threshhold} = 160$ μs.

Inserting Eq. (4) into Eq. (2) yields:

$$M_z = M_0\ exp\left(-\frac{T_2\ BW\ \theta_{ORS}^2}{1 + (2\,\pi\, f_{off}\ T_2)^2}\right) \equiv M_0 Q \tag{5}$$

where Q is introduced to simplify Eq. (5).

Eq. (5) can be inserted into the generalized steady state equation for an SPGR sequence using magnetization preparation with flip angle θ (see for example [11]):

$$S = S_0\ sin\theta\ \frac{1 + (Q-1)\ e^{-T_{spoil}/T1} - Q\ e^{-TR/T1}}{1 - Q\ cos\,\theta_{eff}\ e^{-TR/T1}} \tag{6A}$$

$$\approx S_0\ sin\theta\ Q\frac{1 - e^{-TR/T1}}{1 - Qcos\theta_{eff}\ e^{-TR/T1}} \tag{6B}$$

the last step assuming that the duration of the spoiler gradient T_{spoil} is much less than T1 ($T_{spoil} < < T1$). The effective flip angle θ_{eff} accounts for the fact that the UTE acquisition pulse is applied N times (see Fig. 1A) and is approximately given by $\cos(\theta_{eff}) \approx \cos(\theta)^N$ (ignoring T2 and T1 relaxation during the short durations during and between excitations). The steady state equation (Eqs. (6A) and (6B)) requires prior knowledge of T1 and the UTE excitation flip angle θ. In order to simplify this equation one can employ a long TR (e.g. $TR \gtrsim T1$), and a

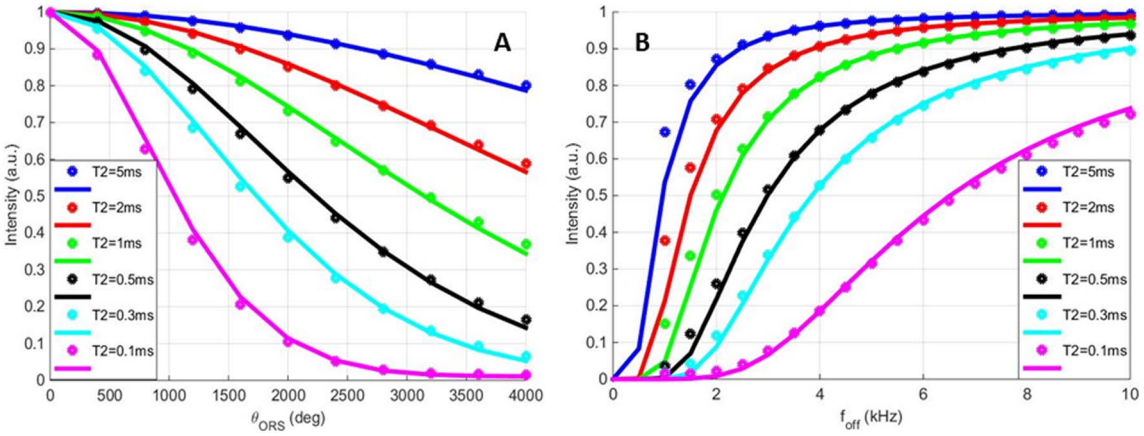

Fig. 2. A) Signal intensity plotted against saturation flip angle θ_{ORS} for different values of T2 (5 ms–0.1 ms). B) Signal intensities plotted against off-resonance frequency f_{off}. The data points are from Bloch simulations while the solid lines correspond to the theoretical curves and show good agreement.

moderately large flip angle so that Eqs. (6A) and (6B) simplifies to:

$$S \approx S_0 \, sin\theta \left(1 - e^{-TR/T1}\right) Q \tag{7}$$

In order to determine T2 from an off-resonance experiment, this can be fitted to the simple signal equation:

$$S \approx AQ + B \tag{8}$$

where the offset B accounts for experimental noise levels as well as the fact that Eq. (6A) does not decrease precisely to zero as Q goes to zero due to T1 recovery during the finite spoiler duration and multi-spoke acquisitions (for $N > 1$).

Eq. (8) was compared to Bloch simulations. Fig. 2A shows the Bloch simulations as well as the theoretical signal curves as a function of saturation flip angle which exhibit the expected Gaussian shapes. Fig. 2B show similar curves as a function of off resonance frequency. Both show good agreement between Bloch simulations and theoretical curves.

Selective positive short T2 contrast can be achieved by subtracting the ORS prepared images from equivalent images without ORS (which are comparatively flat in contrast). The contrast in the subtracted images stems mainly from the saturation images themselves. Fig. 3 shows the theoretical contrast contours using Eq. (5) of ORS prepared signals as a function of saturation RF off-resonance (x-axis) and saturation RF flip angle (y-axis). Highest contrast can be achieved in the red areas. Note that it is more difficult to generate contrast between tendon and muscle, since their approximate T2 values have less separation than the corresponding values for tendon and fat, and fat signals are shifted an additional 440 Hz away from water at 3 T. Hence, their signals may remain high even when the ORS pulse is applied close to the resonance for water because it is further off resonance for fat.

2. Methods

Volunteer imaging was performed on a healthy male volunteer (age 28 yr) using an 8-channel knee coil on a 3T GE HDxt clinical MR scanner. The 3D Cones sequence uses a unique k-space sampling trajectory that samples data along twisting evenly spaced paths on cone surfaces in 3D [12]. It samples data starting from the center of k-space and twists outwards from there with the data acquisition starting as soon as possible after the RF excitation. Both RF and gradient spoiling are used to crush the remaining transverse magnetization after each data acquisition. To study the saturation curves as a function of off-resonance frequencies, the off-resonance saturation preparation was performed using a Fermi RF pulse (duration = 8 ms) with a BW of 160 Hz and flip angle of $\theta_{ORS} = 1500^{\circ}$. Relevant sequence parameters were field of view (FOV) = 20 cm, matrix = 256 × 256, slice thick = 4 mm, UTE RF duration T_{RF} = 70 μs, TE = 30 μs, TR = 300 ms, $N = 10$, $\tau = 4.3$ ms, rBW = 125 kHz, $\theta = 25^{\circ}$, and f_{off} = [−500, 0, 500, 1000, 1500, 2000, 3000, 5000, 10,000, 20,000] Hz. Additionally, a reference scan was performed without application of the ORS pulse. Five small regions of interests (ROIs) were drawn in patella tendon, meniscus, cortical bone, muscle, and bone marrow. T2 values were measured for patella tendon, meniscus, cortical bone, muscle and bone

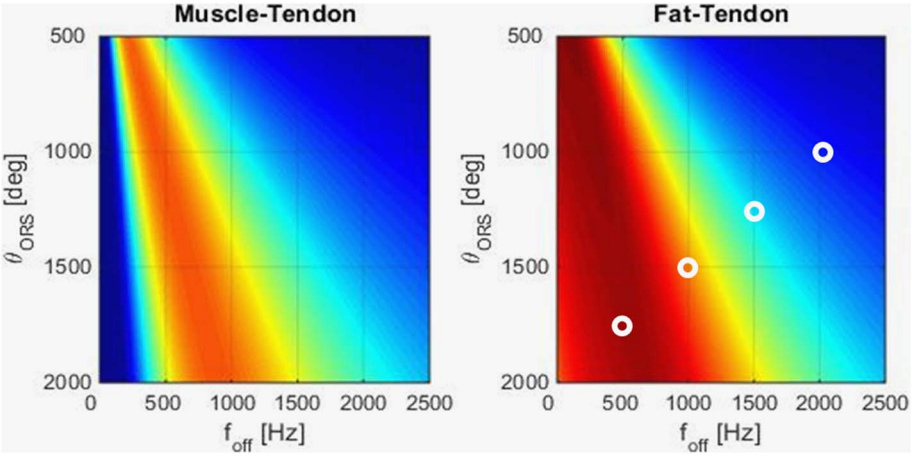

Fig. 3. A): Theoretical contrast curves (S_{longT2}-$S_{shortT2}$) for different values of θ_{ORS} and f_{off} based on Eq. (5), for short T2 contrast of the patella tendon against muscle. B): Equivalent theoretical contrast curves for short T2 contrast of the patella tendon against fat. Also shown are the parameter locations used in the in-vivo experiments shown in Fig. 5.

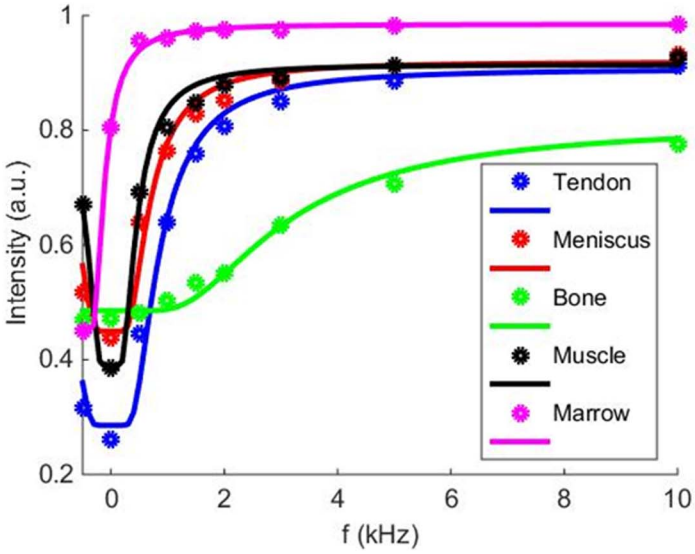

Anatomy	Measured T2 [ms]
Patella Tendon	5.0
Meniscus	7.8
Cortical Bone	0.35
Muscle	17.8
Bone Marrow	35.5

Fig. 4. Experimental signal values (data points) for in-vivo ORS experiments as a function of off-resonance frequency for tendon, meniscus, bone, muscle, and bone marrow. Also shown are the theoretical curve fits to Eq. (8), which match the experimental data (solid lines) reasonably well. The fitted T2 values are shown in table on the right. The values for the short T2 tissues agree well with the values published in the literature [13].

marrow according to Eq. (8).

In order to verify the best parameters (f_{off} and θ_{ORS}) for short T2 contrast optimization, higher resolution scans were performed at several off resonance frequencies and ORS flip angles (f_{off}/θ_{ORS} = 500 Hz/1725°; 1000 Hz/1500°; 1500 Hz/1250°; 2000 Hz/1000°). Relevant sequence parameters were FOV = 15 cm, matrix = 320 × 320, slice thick = 2 mm, UTE RF duration T_{RF} = 70 μs, TE = 30 μs, TR = 200 ms, N = 10, τ = 5.5 ms, rBW = 125 kHz, θ = 10°. Subtraction images were generated by subtracting 3D Cones images with ORS from equivalent 3D Cones images without ORS. Short T2 contrast, defined as $(S_{Fat} - S_{Tendon}) / (S_{Fat} + S_{Tendon})$, was measured for quantitative evaluation.

3. Results

The experimentally measured signal curves in the knee are shown in Fig. 4 as a function of off-resonance frequency. All signals were normalized to the non-ORS signal levels. Shown are both the experimental data and the fitted curves to Eq. (8). Also show next to the figure are the resulting fitted T2 values. The values for the short T2 tissues agree well with values published in the literature [13], however there were deviations for the longer T2 tissues such as muscle and fat.

Fig. 5 shows the high resolution sagittal images of the volunteer's knee. The top panel shows an image with and without ORS. The image without ORS exhibits the expected flat contrast, while the ORS prepared image show the patella tendon with low signal. Also shown is the subtraction of the second image from the first, which generates high positive contrast for the patella tendon. The lower panel shows ORS images using different values of f_{off} and θ_{ORS}. Also displayed are the measured values for the contrast = $(S_{Fat} - S_{Tendon}) / (S_{Fat} + S_{Tendon})$, which agree with the trend predicted by the theoretical results shown in Fig. 3.

4. Discussion

Off-resonance saturation 3D UTE imaging can be used to effectively generate contrast between tissues with long T2 signals and these with short T2 signals. The theoretical equations developed here can be used to determine the ORS sequence parameters such as f_{off} and θ_{ORS} to maximize short T2 contrast. The theoretical model and optimization described in this work could also be used with zero TE (ZTE) imaging [3]. Since dual echo acquisitions are typically not employed in ZTE imaging in order to retain the low acoustic levels, ORS may be particularly useful to generate short T2 contrast in this application.

4.1. Limitations

There are several limitations to our theoretical model:

i. The first limitation is regarding the integration limits in Eq. (4). Here we have assumed a sharp spectral profile of the ORS pulse, but in reality any finite-duration RF pulse has a more rounded spectral response.
ii. In this work, we have exclusively focused on the direct off-resonance saturation of short T2 components and have not included possible effects due to magnetization transfer [10]. In future work, we plan to extend our theoretical framework to include these effects and study the implications towards our optimization model.
iii. Although the short T2 components fit the theoretical model well, there were deviations seen for tissues with longer T2 s such as muscle and fat. While further work has to be conducted, this may be caused by the fact that longer T2 signals exhibit most of their signal drop near resonance, where field inhomogeneities can potentially corrupt quantification. In addition, although our model assumes a single component decay curve, several studies have shown multi-component behaviors of short T2 tissues [14], which are not included in our model.
iv. Finally, since two separate acquisitions have to be collected, the total scan time is typically longer than for a simple dual-echo acquisition. The UTE sequence used in our study has the flexibility to acquire several spokes (N) per ORS application, which greatly reduces the acquisition time and increases the scan efficiency. However, there is a practical limit to N in order to avoid contamination of excessive T1 recovery during the acquisitions of the saturated magnetization. We found that N between 5 and 10 yields a good compromise.

Acknowledgments

Jiang Du was supported by GE Healthcare, the National Institute of Health (1R01 NS092650 and 1R01 AR068987).

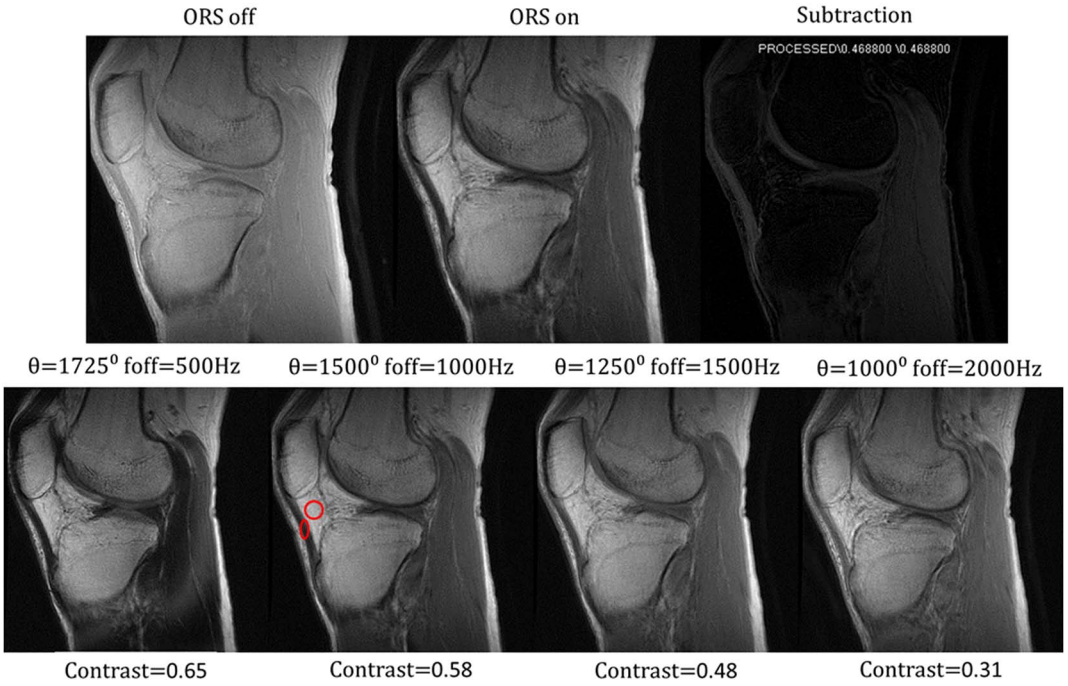

Fig. 5. Upper panel: Sagittal knee images of the volunteer obtained without ORS and with ORS, as well as their subtraction, which shows positive patella tendon signal contrast. Lower panel: ORS prepared images with different values of f_{off} and θ_{ORS} as indicated in Fig. 3. The corresponding values of contrast $(S_{Fat} - S_{Tendon}) / (S_{Fat} + S_{Tendon})$ between fat and tendon (approximate ROI shown in the figure) are also shown. Although the contrast is highest for the case with the smallest off-resonance frequency (left), these images do exhibit some B0 artifacts.

References

[1] Rahmer J, Bornert P, Groen J, Bos C. Three-dimensional radial ultrashort echo-time imaging with T2 adapted sampling. Magn. Reson. Med. 2006;55(5):1075–82.

[2] Du J, Bydder M, Takahashi AM, Carl M, Chung CB, Bydder GM. Short T2 contrast with three-dimensional ultrashort echo time imaging. Magn. Reson. Imaging 2011;29:470–82.

[3] Weiger M, Wu M, Wurnig MC, Kenkel D, Boss A, Andreisek G, et al. ZTE imaging with long-T2 suppression. NMR Biomed. 2015;28(2):247–54.

[4] Li C, Magland JF, Rad HS, Song HK, Wehrli FW. Comparison of optimized soft-tissue suppression schemes for ultrashort Echo time MRI. Magn. Reson. Med. 2012;68(3):680.

[5] Du J, Takahashi A, Bydder M, Chung CB, Bydder GM. Ultrashort TE imaging with off-resonance saturation contrast (UTE-OSC). Magn. Reson. Med. 2009;62:527–31.

[6] Delangre S, Vuong QL, Henrard D, Pob C, Gallez B, Gossuin Y. Bottom-up study of the MRI positive contrast created by the off-resonance saturation sequence. J. Magn. Reson. 2015;254:98–109.

[7] Smith S, Bulte J, Van Zijl P. Direct saturation MRI: theory and application to imaging brain iron. Magn. Reson. Med. 2009;62(2):384–93.

[8] Woessner D, Zhang D, Merritt M, Sherry A. Numerical solution of the Bloch equations provides insights into the optimum design of PARACEST agents for MRI. Magn. Reson. Med. 2005;53:790–9.

[9] Khemtonga C, Togaob O, Renb J, Kessingera C, Takahashib M, Sherryb A, et al. Off-resonance saturation MRI of superparamagnetic nanoprobes: theoretical models and experimental validations. J. Magn. Reson. 2011;209(1):53–60.

[10] Henkelman RM, Huang X, Xiang Q, Stanisz G, Swanson S, Bronskill M. Quantitative interpretation of magnetization transfer. Magn. Reson. Med. 1993;29:759–66.

[11] Carl M, Bydder G, Du J. UTE imaging with simultaneous water and fat signal suppression using a time-efficient multispoke inversion recovery pulse sequence. Magn. Reson. Med. 2016;76:577–82.

[12] Gurney PT, Hargreaves BA, Nishimura DG. Design and analysis of a practical 3D cones trajectory. Magn. Reson. Med. 2006;55:575–82.

[13] Robson MD, Gatehouse PD, Bydder M, Bydder GM. Magnetic resonance: an introduction to ultrashort TE (UTE) imaging. J. Comput. Assist. Tomogr. 2003;27(6):825–46.

[14] Wilhelm MJ, Ong HH, Wehrli SL, Li C, Tsai PH, Hackney DB, et al. Proc. Natl. Acad. Sci. U. S. A. 2012 Jun 12;109(24):9605–10.